



---

## New Discriminant Functions and Geochemistry of the Mamfe Cretaceous Formations (South West Cameroon)

Kenfack Nguemo Gatien Romuald<sup>a\*</sup>, Tematio Paul<sup>b</sup>, Ngueutchoua Gabriel<sup>c</sup>,  
Tata Cathryn Ntoboh<sup>d</sup>, Bokanda Ekoko Eric<sup>e</sup>, Ngounou Kouokam Annyck  
Channele<sup>f</sup>, Wabo Hervéa<sup>g</sup>, Tcheumenak Kouemo Jules<sup>h</sup>, Momo Nouazi  
Mathieu<sup>i</sup>

<sup>a,b,f,h,i</sup>University of Dschang, PO BOX, 67, Dschang, Cameroon

<sup>c,d,e</sup>University of Yaoundé I, Cameroon

<sup>g</sup>University of Johannesburg, South Africa

<sup>a</sup>Email: [kenngatien@yahoo.fr](mailto:kenngatien@yahoo.fr)

<sup>a</sup>Email: [paul\\_tematio@yahoo.fr](mailto:paul_tematio@yahoo.fr)

### Abstract

Major and trace element geochemistry have been used to unravel the tectonic setting, source rock composition, and depositional environment of sedimentary rocks in the Mamfe formation. Field studies reveal both sub tabular and tabular outcrops indicating a post tectonic sedimentary activity for the subtabular outcrops. Major element geochemistry reveals a moderate to high proportion (50-75wt %) of silica for the analyzed samples. New discriminant diagrams constructed for usage of adjusted major elements shows samples plotting on collision, arc and rift. Another discriminant plot for adjusted major element combined with trace elements shows samples plotting on active and passive tectonic setting. Ratios of highly immobile trace elements such as Cr/Th, Th/Sc, Th/Co, and La/Sc conclude a felsic source rock for the studied rocks of the Mamfe formation. Trace elements ratios for redox conditions and marine-continental discrimination such as Ni/Co, U/Th, V/Cr, Th/U, and Y/Ho show that the sedimentary rocks of the formation were deposited in a shallow oxygenated continental fluvio-lacustrine environment.

**Keywords:** Mamfe basin; Geochemistry; Fluvio-lacustrine; Active and Passive margins.

---

\* Corresponding author.

## **1. Introduction**

The weathering of preexisting igneous and metamorphic rocks leads to the formation of sediments. These sediments parked in a junk may undergo sedimentary differentiation leading to the different sedimentary rocks. This differentiation is affected by factors such as the velocity of the transporting medium, mode and agent transportation, and, environment of deposition. Detrital sedimentary rocks enclose essential evidence about changes in the supply of material from diverse sources over time, and the geochemical compositions of such sediments have demonstrated to be a prevailing tool for rebuilding the signature of tectonic settings, the composition of the source areas and the provenance of the sediments. Most authors have used the traditional method of petrography to decipher the tectonic setting and source rock composition of medium to very coarse grained sediment by using ternary diagrams provided by [1], and diamond diagram provided by [2]. The petrographic methods recently used by [3] are unclear as the geochemical and mineralogical composition of these sediments are from time to time influenced by processes in the course of transportation, sedimentation and diagenesis. Trace elements and rare earth elements (REE) are thought to be useful signs of provenance, and tectonic setting owing to their reasonably low mobility and insolubility throughout sedimentary processes. The determination of the tectonic setting of sediments have been sorted mostly by discriminants and ternary diagram proposed by [4,5], although countless studies on sediment geochemistry designate that these diagrams do not perform suitably [6,7,8,9]. This work seeks to decipher the tectonic setting, source rock composition and depositional environment of the sedimentary rocks of the Mamfe formations in the Mamfe basin.

## **2. Geologic setting and stratigraphy**

The Mamfe sedimentary basin situated in West Africa lies between longitude of East 8° 00' to 90° 30' and latitude of North 5° 30' to 6° 30'(Figure 1). This basin has been described as a rift splay which is genetically linked to the Benue trough.

The rift is thought to be form from the reactivation of the E-W Mylonitic zone within the Pan African basement [10,11] related the formation of this basin to the opening of the South Atlantic Ocean, associated to the drifting of the Gondwanaland followed by the separation of the Africa plate from the South American plate.

Reference [12] deduced the presence of clastic dykes and soft sediments deformation structures within this basin. He concluded that these clastic dykes are extrusive, formed from tectonovolcanic activities. His assumptions were based on the concomitant plunging angle of the clastic dykes and the magmatic dykes and the non-discordant nature of the clastic dykes and the basement rocks. This basin is believed to be composed predominantly of continental sediments consisting mainly of conglomerate, arkosic sandstone, mudstone, limestone, and evaporates [3,13].

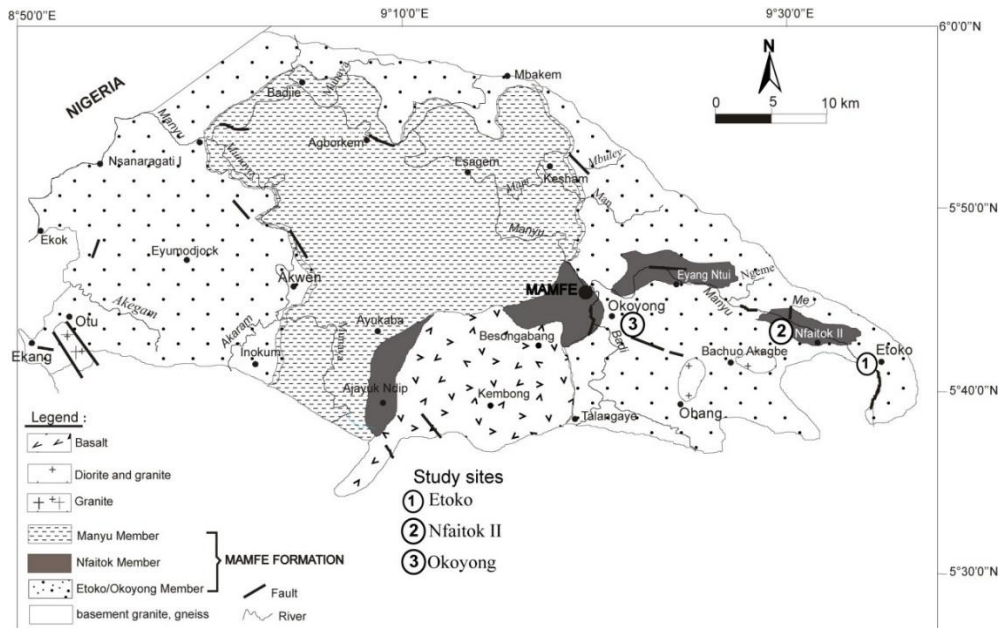


**Figure 1:** Simplified geologic map of the Mamfe Basin showing the study areas modified from [15].

Stratigraphically, Reference [14] documented five series of sedimentary rocks in the Eastern part of the Mamfe basin from bottom to top as the: Manyu sandy clay and Lower conglomeratic sandstone series, Upper conglomeratic sandstone series, Clayey sandstone series, Cross River sandstone series. Reference [10] reviewed the five series propose by [14] into four stratigraphic formations, which are from top to base as the: Cross River formations, Baso, Ngeme, Nfaitok with each subdivided into different members. Reference [15] clustered the sedimentary facies of the basin into the Mamfe formation, which he sub-divided into the Etoko-okoyong, Nfaitok and Manyu members, all underlain by Precambrian basement rock (Figure.2).

Lithology	Age	FORMATION	MEMBER
	Tertiary	MAMFE	MANYU
	Cenomanian		
	Albian		NFAITOK
	Aptian		
	Berremian-Pre-Berremian		ETOKO-OKOYONG
	Pre-Cambrian		

**Figure 2:** Generalized stratigraphic framework of the Mamfe Basin[15]

### **3. Material and Methodology**

The methodology approached used in this worked were grouped in to field and laboratory studies. Field studies entails the identification of the different sedimentary facies, while describing their physical feature such as color, texture, structure and dilute acid reaction. In the laboratory 14 samples of mixed shales and sandstones were performed for geochemical analysis. Fresh samples harvested from surface outcrops were crushed to powder at the institute of mining and geological research, Cameroon (IRGM). Samples were collected from road cuttings and river beds outcrops. The 14 samples were analyzed for major, trace and rare earth elements contents by x ray fluorescence (XRF) and inductively coupled plasma– mass spectrometry (ICP–MS) at the mineral laboratory at Vancouver university, British Columbia, Canada. Standard sample preparation and analytical techniques were used following procedures used in [13] for ICP-MS analyses [16] for XRF analyses. For XRF, 0.2g powdered samples were mixed with sodium metaborate and lithium metaborate of 0.9g. the mixture was put in a furnace of 1000oC. The liquid was allowed to cool and then redissolve in 100ml nitric acid at 4% and hydrochloric acid at 2%. The results after passing the solution through x ray fluorescence were corrected to avoid spectral interference of elements. For ICPMS, 0,5g of the samples were first treated with dilute nitric acid to react with any carbonate, then evaporated to dryness followed by dissolution in a nitric-hydrofluoric acid mix. The samples were evaporated to dryness and concentrated nitric and hydrofluoric acid was added to them three times over three days. The samples were then dissolve again in a 2% nitric double distilled water solution and diluted to 1000 times for MS. The USGS standards were run for calibration and accuracy was generally within 10% and precision 5%. For tectonic setting, new methods discriminant functions of [8] will be used. The new method proposed [9], concentrated on major element. Samples with adjusted silica ( $(SiO_2)_{adj}$ ) between 35% and 95% were subdivided into high-silica and low-silica groups (Table 2). The subscript adj in  $(SiO_2)_{adj}$  refers to the  $SiO_2$  value obtained after volatile-free adjustment of the ten major-elements to 100 wt.%, with the prior conversion of reported Fe concentration ( $FeO$  or  $Fe_2O_3$ ) as  $Fe_2O_3t$  (total Fe) from appropriate atomic or molecular weights. This adjustment ascertained an identical treatment to all samples and standardized the future use of the proposed diagrams. After all adjustment, the discriminant functions ( $DF_1$  and  $DF_2$ ) of the sediments were calculated differently for both sediments of low and high silica. The formulas used in these work retrieved from [8] are seen in table1. In the work of [9], the same method was used for major and trace elements adjustment. This method added the calculation of the isometric log ratio of the elements in the sediments and calculated only one discriminant functions for major elements ( $DF(A-P)M$ ) and major elements combine with trace elements ( $DF(A-P)MT$ ) as seen in table 2. For better understanding in using these methods see supplementary sheets of [8]. For the source rock composition, ratios for ranges of trace elements like  $Cr/Th$ ,  $Th/Sc$ ,  $Th/Co$ , and  $La/Sc$  will be used in this work, whereas for depositional environment and conditions interpretation, the different sedimentary facies recognized on the field will be associated following [17,18,19] to ascertained the depositional environment, while Trace elements ratios such  $Th/U$ ,  $U/Th$ ,  $Ni/Co$ , and,  $V/Cr$  [20, 21, 22] will be used to decipher depositional conditions.

**Table 1:** Discriminant function equations for new discrimination diagrams using major elements

Group names	Silica proportion ranges for calculation of discriminant functions
<b>Arc-Rift-Col</b>	<b>For low silica (&gt;35%-≤ 63%)</b> <b>DF1</b> = (0.608×ln(TiO <sub>2</sub> /SiO <sub>2</sub> )adj)+ (-1.854×ln(Al <sub>2</sub> O <sub>3</sub> /SiO <sub>2</sub> )adj)+ (0.299×ln(Fe <sub>2</sub> O <sub>3t</sub> /SiO <sub>2</sub> )adj)+ (-0.550×ln(MnO/SiO <sub>2</sub> )adj)+ (0.120×ln(MgO/SiO <sub>2</sub> )adj)+ (0.194×ln(CaO/SiO <sub>2</sub> )adj)+ (-1.510×ln(Na <sub>2</sub> O/SiO <sub>2</sub> )adj)+ (1.94×ln(K <sub>2</sub> O/SiO <sub>2</sub> )adj)+ (0.003×ln(P <sub>2</sub> O <sub>5</sub> /SiO <sub>2</sub> )adj)-0.294. <b>DF2</b> = (-0.554×ln(TiO <sub>2</sub> /SiO <sub>2</sub> )adj)+ (-0.995×ln(Al <sub>2</sub> O <sub>3</sub> /SiO <sub>2</sub> )adj)+ (1.765×ln(Fe <sub>2</sub> O <sub>3t</sub> /SiO <sub>2</sub> )adj)+ (-1.391×ln(MnO/SiO <sub>2</sub> )adj)+ (-0.034×ln(MgO/SiO <sub>2</sub> )adj)+ (0.225×ln(CaO/SiO <sub>2</sub> )adj)+ (0.713×ln(Na <sub>2</sub> O/SiO <sub>2</sub> )adj)+ (0.330×ln(K <sub>2</sub> O/SiO <sub>2</sub> )adj)+ (0.637×ln(P <sub>2</sub> O <sub>5</sub> /SiO <sub>2</sub> )adj)-3.631
<b>Arc-Rift-Col</b>	<b>For high silica (&gt;63%-≤ 95%)</b> <b>DF1</b> = (-0.263×ln(TiO <sub>2</sub> /SiO <sub>2</sub> )adj)+ (0.604×ln(Al <sub>2</sub> O <sub>3</sub> /SiO <sub>2</sub> )adj)+ (-1.725×ln(Fe <sub>2</sub> O <sub>3t</sub> /SiO <sub>2</sub> )adj)+ (0.660×ln(MnO/SiO <sub>2</sub> )adj)+ (2.191×ln(MgO/SiO <sub>2</sub> )adj)+ (0.144×ln(CaO/SiO <sub>2</sub> )adj)+ (-1.304×ln(Na <sub>2</sub> O/SiO <sub>2</sub> )adj)+ (0.054×ln(K <sub>2</sub> O/SiO <sub>2</sub> )adj)+ (-0.330×ln(P <sub>2</sub> O <sub>5</sub> /SiO <sub>2</sub> )adj)+1.588 <b>DF2</b> = (-1.196×ln(TiO <sub>2</sub> /SiO <sub>2</sub> )adj)+ (-1.064×ln(Al <sub>2</sub> O <sub>3</sub> /SiO <sub>2</sub> )adj)+ (0.303×ln(Fe <sub>2</sub> O <sub>3t</sub> /SiO <sub>2</sub> )adj)+ (0.436×ln(MnO/SiO <sub>2</sub> )adj)+ (0.838×ln(MgO/SiO <sub>2</sub> )adj)+ (-0.407×ln(CaO/SiO <sub>2</sub> )adj)+ (1.021×ln(Na <sub>2</sub> O/SiO <sub>2</sub> )adj)+ (-1.706×ln(K <sub>2</sub> O/SiO <sub>2</sub> )adj)+ (-0.126×ln(P <sub>2</sub> O <sub>5</sub> /SiO <sub>2</sub> )adj)-1.068

**Table 2:** Discriminant function equations for new discrimination diagrams using major elements and trace

Name	Calculation of discriminant functions
<b>A-P</b>	<b>DF<sub>(A-P)M</sub></b> = (3.0005×llr1 <sub>TiM</sub> ) + (2.8243×llr2 <sub>AlM</sub> ) + (-1.596×llr3 <sub>FeM</sub> ) + (-0.7056×llr4 <sub>MnM</sub> ) + (-0.3044×llr5 <sub>MgM</sub> ) + (0.6277×llr6 <sub>CaM</sub> ) + (-1.1838×llr7 <sub>NaM</sub> ) + (1.5915×llr8 <sub>KM</sub> ) + (0.1526×llr9 <sub>PM</sub> ) -5.9948  <b>DF<sub>(A-P)MT</sub></b> = (3.2683×llr1 <sub>TiMT</sub> ) + (5.3873×llr2 <sub>AlMT</sub> ) + (1.5546×llr3 <sub>FeMT</sub> ) + (3.2166×llr4 <sub>MnMT</sub> ) + (4.7542×llr5 <sub>MgMT</sub> ) + (2.0390×llr6 <sub>CaMT</sub> ) + (4.0490×llr7 <sub>NaMT</sub> ) + (3.1505×llr8 <sub>KMT</sub> ) + (2.3688×llr9 <sub>PMT</sub> ) + (2.8354×llr10 <sub>CrMT</sub> ) + (0.9011×llr11 <sub>NbMT</sub> ) + (1.9128×llr12 <sub>NiMT</sub> ) + (2.9094×llr13 <sub>VMT</sub> ) + (4.1507×llr14 <sub>YMT</sub> ) + (3.4871×llr15 <sub>ZrMT</sub> ) -3.2088

## 4. Results

### 4.1 Field description

Figure. 3 presents outcrops from where analyzed rocks were sampled. These rocks were collected at Etoko-Yawo, Nfaitock River, Okoyong. Their variable characteristics are described below.

#### 4.1.1 Etoko Yawo site 1

The outcrop at Etoko has a thickness of 7 meters. The rocks display a steep like tabular structure striking N170E with a dip angle of 01° to the SW direction at Yawo. The facies present are sandstones, shales and conglomerates. Conglomerate are matrix supported to clast supported with clast size ranging from pebble to boulders. Most of the clast are composed of granite, gneiss, quartzites and mica schist (Figure. 3a). The dark grey to black shales are interbedded with whitish sandstones of medium grain sizes (Figure. 3b).

#### 4.1.2 Nfaitok site 2

At Nfaitok the outcrop displays a sub-tabular nature with a striking direction of N120E dipping 10NE at Nfaitok river (Figure. 3c). The facies present are dark grey sandstones and black shales. The dark grey sandstones alongside the black shales reacts vigorously with dilute HCl indicating the presence of carbonates minerals. The sandstones are medium grained whereas the shales display a very fine grained texture. The succession shows an interbedding of sandstones and shales.

#### 4.1.3 Okoyong site 3

The outcrop in Okoyong (Figure. 3b) comprise predominantly of very coarse-grained sandstones with intercalation of shale and conglomerate. Generally, the outcrop appears to be sub-tabular striking N170E with a 20° dip angle to the SW. The conglomerates exhibit pebble size clast bounded held together by a sandy matrix. The clast composition of the conglomerate is mostly quartzite.

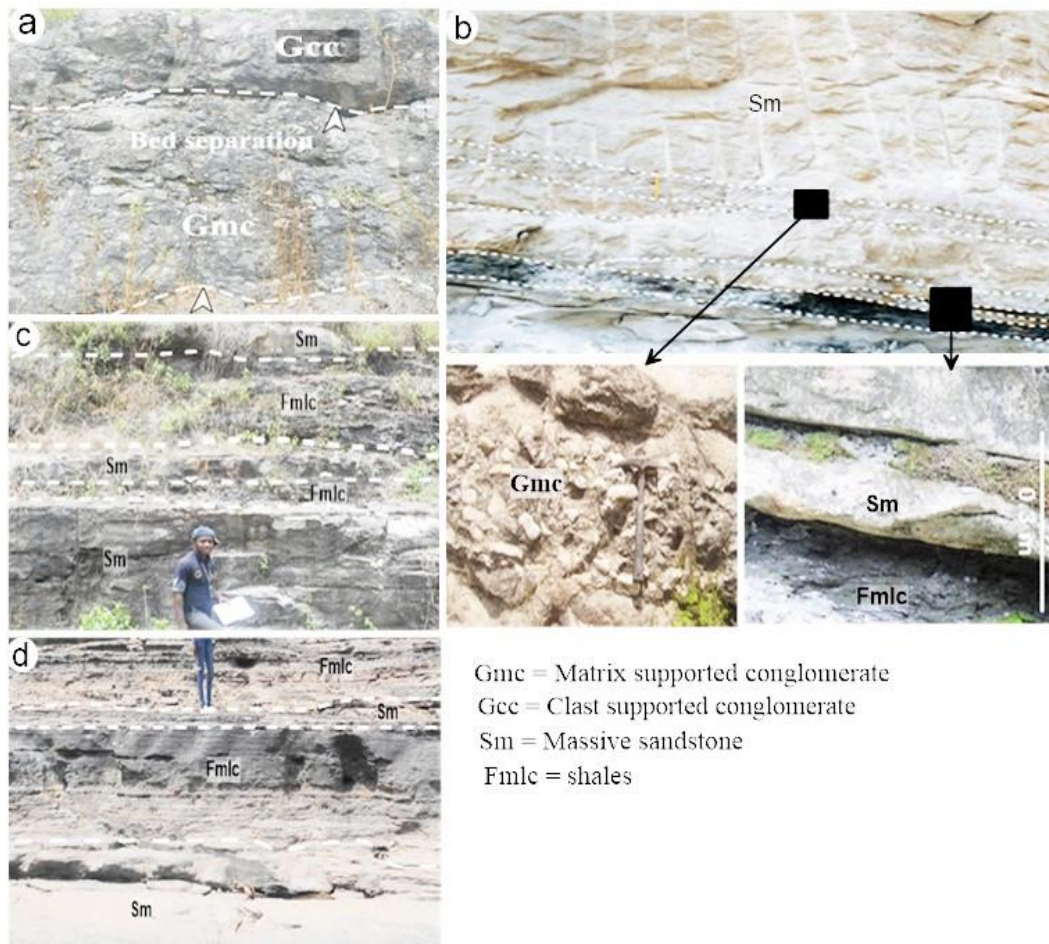


**Figure 3:** Field photographs of studied outcrops. (a) Site 1, Matrix to clast supported conglomerate, (b) tabular dark grey shales intercalated with fine grained whitish sandstones. (c) Site 3, sub-tabular black shales intercalated with fine grained massive sandstones and matrix supported conglomerate. (d) Site 2, sub-tabular calcareous banded black shales interbedded with massive dark grey sandstones.

## **4.2 Geochemical description**

Table 3 presents data for adjusted major elements and table 4 constitute data for trace elements and their calculated ratio for rock samples collected at Etoko-Yawo, Nfaiok, Okoyong.

### **4.2.1 Etoko Yawo site 1**

Four samples were analyzed on this have a high proportion of silica ranging between 50 and 73 wt% after anhydrous adjustment (Table 3).

The Al<sub>2</sub>O<sub>3</sub> proportion of the samples in this site ranges between 10 and 13.5wt% with an average of 13.16wt% being almost equal the average value of samples analyzed in Okoyong site 3 (13.36wt%).

Trace elements ratios of Ni/Co, U/Th, V/Cr, Th/U and Y/Ho have average values of 2.36, 0.37, 3.1, 3.01, and 30.07 respectively. Ratios of trace elements such as Th/Cr, La/Sc, Th/sc, Th/Co and Cr/Th for the studied samples on average have 0.63, 7.37, 1.89, 1.26, and 2.86 respectively (Table 4).

### **4.2.2 Nfaiok site 2**

Six samples were analyzed on this site have an average to high proportion of silica ranging between 50 and 75 wt% after anhydrous adjustment (Table 3). The Al<sub>2</sub>O<sub>3</sub> proportion of the samples in this site ranges between 10 and 15wt% with an average of 13.2w% being almost equal the average value of samples analyzed in Etoko site 1 and Okoyong site 3 (13.36wt%).

Trace elements ratios of Ni/Co, U/Th, V/Cr, Th/U and Y/Ho have average values of 2.15, 0.31, 3.2, 3.52 and 28.04 respectively. Ratios of trace elements such as Th/Cr, La/Sc, Th/sc, Th/Co and Cr/Th for the studied samples on average have 0.67, 7.74, 1.92, 1.15, and 3.42 respectively (Table 4).

### **4.3.3 Okoyong site 3**

Four samples were analyzed generally on this site with OK1 and OK19 having a higher silica proportion as compared to OK7 and OK11 after anhydrous adjustment (Table 3). Samples of OK1 and OK19 are sandstones while the OK7 and OK11 are shales.

Trace elements ratios of Ni/Co, U/Th, V/Cr, Th/U and Y/Ho have average values of 3.0, 0.27, 2.66, 3.88 and 28.81 respectively. Ratios of trace elements such as Th/Cr, La/Sc, Th/sc, Th/Co and Cr/Th for the studied samples on average have 0.45, 6.51, 1.77, 1.05, and 4.25 respectively (Table 4).

**Table 3:** Adjusted major elements (wt%) and their calculated discriminant functions

	Etoko				Nfaitok						Okoyong			
	ET1	ET2	ET3	ET4	FA1	FA2	FA3	FA4	FA5	FA6	OK1	OK2	OK3	OK4
(SiO <sub>2</sub> )adj	50.9	73.7	60.6	63.9	52.3	75.9	56.0	56.0	53.0	64.9	46.2	77.4	54.9	76.9
(TiO <sub>2</sub> )adj	0.6	0.4	0.6	0.6	0.5	0.3	0.9	0.9	1.0	0.7	0.4	0.3	1.5	0.9
(Al <sub>2</sub> O <sub>3</sub> )adj	13.2	14.1	15.1	14.5	12.9	13.9	16.6	16.6	17.4	14.6	8.7	12.7	27.1	10.4
(Fe <sub>2</sub> O <sub>3</sub> )adj	5.3	2.1	6.3	4.2	6.8	0.7	6.9	6.9	8.5	4.0	14.6	1.4	4.6	3.9
(MnO)adj	0.4	0.0	0.2	0.2	1.1	0.2	0.2	0.2	0.2	0.2	1.4	0.0	0.0	0.1
(MgO)adj	10.9	1.5	3.0	3.4	3.6	0.1	3.9	3.9	4.0	3.0	19.0	0.6	3.2	2.1
(CaO)adj	12.3	0.7	6.6	5.8	15.7	0.3	8.2	8.2	7.7	5.1	3.1	1.0	0.7	0.5
(Na <sub>2</sub> O)adj	2.5	3.4	3.8	3.9	4.2	5.4	4.0	4.0	5.2	4.3	0.4	2.4	0.4	1.7
(K <sub>2</sub> O)adj	3.7	4.0	3.5	3.3	2.2	3.1	3.2	3.2	2.7	2.9	5.4	4.0	7.3	3.4
(P <sub>2</sub> O <sub>5</sub> )adj	0.2	0.2	0.2	0.2	0.7	0.2	0.2	0.2	0.3	0.2	1.0	0.1	0.3	0.1
ln(TiO <sub>2</sub> /SiO <sub>2</sub> )adj	-4.4	-5.3	-4.5	-4.7	-4.7	-5.6	-4.1	-4.1	-4.0	-4.6	-4.7	-5.7	-3.6	-4.5
ln(Al <sub>2</sub> O <sub>3</sub> /SiO <sub>2</sub> )adj	-1.3	-1.7	-1.4	-1.5	-1.4	-1.7	-1.2	-1.2	-1.1	-1.5	-1.7	-1.8	-0.7	-2.0
ln(Fe <sub>2</sub> O <sub>3</sub> /SiO <sub>2</sub> )adj	-2.3	-3.6	-2.3	-2.7	-2.0	-4.7	-2.1	-2.1	-1.8	-2.8	-1.2	-4.0	-2.5	-3.0
ln(MnO/SiO <sub>2</sub> )adj	-5.0	-8.9	-5.9	-5.8	-3.9	-6.1	-5.6	-5.6	-5.9	-6.0	-3.5	-8.9	-7.1	-7.1
ln(MgO/SiO <sub>2</sub> )adj	-1.5	-3.9	-3.0	-2.9	-2.7	-6.8	-2.7	-2.7	-2.6	-3.1	-0.9	-4.8	-2.8	-3.6
ln(CaO/SiO <sub>2</sub> )adj	-1.4	-4.7	-2.2	-2.4	-1.2	-5.4	-1.9	-1.9	-1.9	-2.5	-2.7	-4.3	-4.3	-5.1
ln(Na <sub>2</sub> O/SiO <sub>2</sub> )adj	-3.0	-3.1	-2.8	-2.8	-2.5	-2.6	-2.6	-2.6	-2.3	-2.7	-4.6	-3.5	-4.9	-3.8
ln(K <sub>2</sub> O/SiO <sub>2</sub> )adj	-2.6	-2.9	-2.8	-3.0	-3.2	-3.2	-2.9	-2.9	-3.0	-3.1	-2.2	-3.0	-2.0	-3.1
ln(P <sub>2</sub> O <sub>5</sub> /SiO <sub>2</sub> )adj	-5.4	-6.2	-5.7	-5.8	-4.3	-6.2	-5.6	-5.6	-5.3	-6.0	-3.9	-6.5	-5.3	-6.3
DF1	-2.2	-3.9	-3.3	-3.6	-4.1	-6.1	-3.5	-3.5	-4.2	-4.0	1.7	-3.6	0.4	-2.0
DF2	-1.8	3.2	0.8	-0.2	-0.7	0.5	0.1	0.1	1.1	0.0	-2.4	3.4	-0.8	0.6

**Table 4:** Trace elements (ppm) and their calculated ratio

	Etoko-Yawo				Nfaitok						Okoyong			
	ET1	ET2	ET3	ET4	FA1	FA2	FA3	FA4	FA5	FA6	OK1	OK2	OK3	OK4
Cr	20	30	20	30	20	40	30	30	20	40	50	30	20	30
Th	10.8	9	15.74	18.23	21.6	3.6	20.6	17.9	27.5	8.6	11.3	7.05	24.1	4
U	4.7	5.3	6.7	7.17	8.7	1.1	3.3	5.9	10.7	2.4	4.3	1.4	7.1	0.9
V	66	36	82.3	95.33	55	18	112	83	145	92	60	23	158	23
Y	18.7	13.1	21.23	32.5	35.5	23.1	43.3	18.3	37.9	21.1	26.2	11.9	55.8	13.3
Ni	28	15	31.1	27.33	28	19	47	30	47	10	120	19	41	24
Co	14.9	3.4	12.6	13.83	13.7	7.4	17.3	13.2	22.8	8	65.5	4.2	12.2	10.6
Ho	0.69	0.47	0.76	0.75	1.18	0.82	1.42	0.65	1.37	0.73	0.79	0.42	2.02	0.48
La	37	50.2	65.3	49.7	95.9	16.2	83.2	66.3	100	48.7	49.6	22.6	118.5	17.9
Sc	8	4	8.57	9.57	6	5	12	7	14	9	5	3	21	3
Cr/Th	1.85	3.33	1.27	1.65	0.93	11.11	1.46	1.68	0.73	4.65	4.42	4.26	0.83	7.5
V/Cr	3.3	1.2	4.12	3.18	2.75	0.45	3.73	2.77	7.25	2.3	1.2	0.77	7.9	0.77
Th/Cr	0.54	0.3	0.79	0.61	1.08	0.09	0.69	0.6	1.38	0.22	0.23	0.24	1.21	0.13
Th/U	2.3	1.7	2.35	2.54	2.48	3.27	6.24	3.03	2.57	3.58	2.63	5.04	3.39	4.44
Th/Co	0.72	2.65	1.25	1.32	1.58	0.49	1.19	1.36	1.21	1.08	0.17	1.68	1.98	0.38
Th/Sc	1.35	2.25	1.84	1.9	3.6	0.72	1.72	2.56	1.96	0.96	2.26	2.35	1.15	1.33

<b>U/Th</b>	0.44	0.59	0.43	0.39	0.4	0.31	0.16	0.33	0.39	0.28	0.38	0.2	0.29	0.23
<b>Ni/Co</b>	1.88	4.41	2.47	1.98	2.04	2.57	2.72	2.27	2.06	1.25	1.83	4.52	3.36	2.26
<b>Y/Ni</b>	0.67	0.87	0.68	1.19	1.27	1.22	0.92	0.61	0.81	2.11	0.22	0.63	1.36	0.55
<b>La/Sc</b>	4.6	12.6	7.6	5.2	0.36	2.22	0.27	0.36	0.14	33.2	9.9	7.5	5.6	6.0
<b>Y/Ho</b>	27.1	27.9	27.9	43.3	30.1	28.2	30.5	28.2	27.7	28.9	28.3	27.6	27.7	28.8

## 5. Discussion

### 5.1 New discriminant diagrams and tectonic setting

[8,9] emphasizes on the usage of the new discriminant function to decipher the tectonic setting of the settings of sediments. These new methods from several test performed by them has a higher chance as compared to the old diagrams used by [5,6]. Due to this facts, [27] proposed that the realization of the plate tectonic settings of sedimentary rocks using diagrams [5][6] are unsatisfactory because it does not incorporate a coherent statistical treatment of composition[23]. Also, the discrimination diagrams [6] were unable to differentiate arc sediments from those of continental rift and collision. From discriminant diagrams [8,9] the studied rocks from the Mamfe formations plots in the domain of arc, collision, and rift (Figure 4a, b). Also, in Figure.5, the samples plot in the domain of passive with some falling within the domain of active margin (Figure 5a, b). The collision, arc and active tectonic setting with respect to the geology of Africa and Cameroon in particular seems impossible due to their passive margin tectonic characteristic. However, there are possibilities that the samples which were plotted in the collision, arc and active field reflect the complex history of the Pan African orogeny. This orogeny was a tectono-thermal event, some 500Ma ago, resulting in the opening and closure of large Proterozoic oceanic realms as well as accretion and collision of buoyant crustal blocks [24].

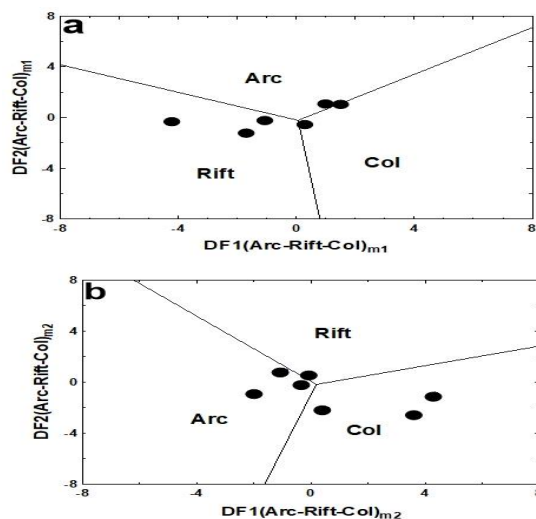


**Figure 4:** (a) New discriminant-function multi-dimensional diagram for high-silica clastic sediments from three tectonic settings (arc, continental, rift, and collision), (b) New discriminant-function multi-dimensional diagram for low-silica clastic sediments from three tectonic settings (arc, continental rift, and collision) [8].

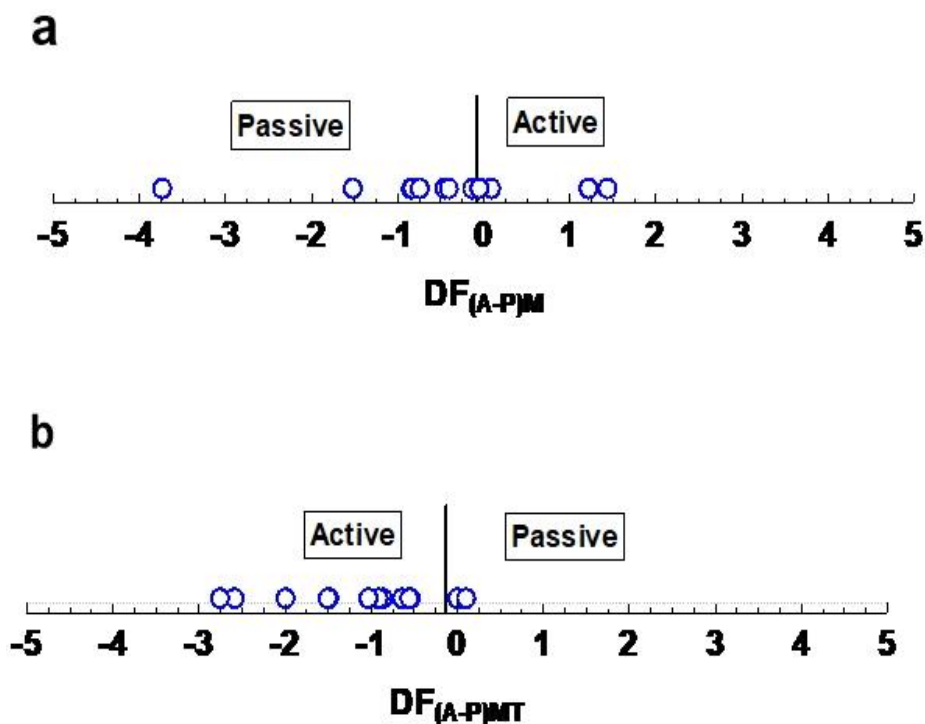


**Figure 5:** (a) New major element (M) based multidimensional discriminant function diagram for the discrimination of active (A) and passive (P) margin settings. (b) New combined major and trace element (MT) based multidimensional discriminant function diagram for the discrimination of active (A) and passive (P) margin settings after [9].

The Pan-African belt in central Africa (Cameroon) consists of Neoproterozoic supracrustal assemblage, deformed granitoids, and medium- to high-grade Neoproterozoic metamorphic rocks, which are interpreted to have formed in a continental collision zone [24][25]. This suggestion visualizes an ancient collisional setting for the source rocks and implies the relative importance of the source areas in controlling the composition of the studied sediments.

### 5.2 Trace elements ratios and source rock composition

According to [26], nickel and chromium proportions in sedimentary rocks may be used to depict their source rock composition. To him, Ni and Cr proportions inferior to 100 ppm and inferior to 150 ppm respectively specifies a felsic source rock composition. The proportion of the studied samples are inferior to 100 and 150 ppm for Ni (For study samples; Ni=) and Cr (For study samples; Cr=) respectively thus, implying a felsic source rock provenance. According to [27], the La/Sc and Th/Sc ratios of mafic sediments are always inferior to sediments derived from mafic rocks.

Reference [28] denotes that, the ratios of relatively immobile trace elements such as Cr/Th, Th/Sc, Th/Co, and La/Sc appropriate indicators of determining source rock composition of sedimentary rocks. The ratios of these elements resulting from mafic, and felsic sediments judge against those of the present study (Table 5) confirms that our data are inside the range of felsic source rocks.

**Table 5:** Trace element calculated ratios of the studied sites

	Mamfe formation samples <sup>1</sup>			Range of sediments <sup>2</sup>	
	Site 1avg (n=4)	Site 2avg(n=6)	Site 3avg(n=4)	Felsic	Mafic
<b>Th/Cr</b>	0.63	0.67	0.45	0.13-2.7	0.018-0.046
<b>La/Sc</b>	7.73	7.74	6.51	2.51-16.3	0.43-0.86
<b>Th/Sc</b>	1.89	1.92	1.77	0.84-20.5	0.05-0.22
<b>Th/Co</b>	1.23	1.15	1.05	0.67-19.4	0.04-1.4
<b>Cr/Th</b>	2.89	3.42	4.25	4.0-15.0	25-500

<sup>1</sup>This study, <sup>2</sup>(Cullers 2002), avg=average

### 5.3 Field and depositional environment

Outcrops observe in the field display dissimilarities in their structural occurrence with some being tabular and others sub-tabular. This dissimilarity may signpost post-deposition tectonic activity for the sub-tabular outcrops, which may justify a changes in their depositional environment when compared to the tabular outcrops that may have been probably deposited after the tectonic interval [17,18,19] used facies association to decipher the depositional setting of sedimentary rocks within sedimentary basins. The presence of poorly sorted clast to matrix supported conglomerates associated with non bioturbated medium to coarse grained sandstones in the study area signpost a fluvial channel depositional setting [18,19]. The dark grey to black carboniferous shales with organic matter may results from accumulation of plant materials and clay in stable conditions signposting a coastal swamp environment. This environment suggest low energy condition associated to low sedimentation rates [18]. The distinct horizontal orientation coupled with lateral continuity, dark grey to black color, very fine – fine grained and calcareous composition of the shales in the study area signpost a lacustrine depositional setting [13]. Nonetheless, the depositional environment determined above cannot be precisely decided from field characteristics. The geochemical analysis presented in this work will enhance valuable evidence towards establishing the depositional settings.

### 5.4 Trace elements and depositional environment

Vanadium, Ni, U, Co, and Th are sensitive to redox conditions [21,22,29,30,31] and their ratios permit the understanding of the depositional conditions of sediments. According to plots from [13] developed from trace elements ratio, most of the studied samples were deposited in an oxic environment. The Ni/Co plots used [12] compared to the ratios of studied samples also signpost oxic conditions at the time of their deposition. Abigail and his colleagues [31] disclose a strongly Y/Ho ratio (elemental Y/Ho 40–90) for Phanerozoic seawater. Bokanda and his colleagues [13] proposed that, the Th/U >2 depicts continental environments while Th/U ratio of less than 2 disclose a marine environment. Compositionally the studied samples are distinguishable from those of the Phanerozoic seawater as they have a weak positive to average chondrite Y/Ho ratio (29.7, n=25) and also a Th/U ratio of >2. The unsatisfactory similarity of the studied samples to marine Y/Ho dismisses a marine influence on their depositional settings whereas their Th/U ratio confirms a continental influence for

their deposition setting.

## **6. Conclusion**

The major and trace elements geochemical results of the studied sedimentary facies unveil the following conclusions:

- (1) The studied outcrops exhibit variable structural dip directions signifying that post sedimentary tectonic activity affected some of the studied outcrops. This may denote a time gap between non-tectonized and tectonized outcrops.
- (2) The samples signpost a passive and active tectonic setting from new discriminant function diagram and disclose a felsic parent rock composition from trace element ratios of Cr/Th, Th/Sc, Th/Co, and La/Sc.
- (3) The outcrops of study area disclose conglomerate, sandstones and shales of variable characteristics disclosing a fluvial and highly vegetated lacustrine swamp depositional environment setting.
- (5) The continental fluvial and lacustrine environment may have probably been some elevated areas in the sedimentary basin. This is based on the presence of oxic conditions inferred from trace elements ratios of U/Th, Ni/Co and V/Cr.

## **Acknowledgments**

The authors grateful to Dr Armstrong-Altrin and professor Surendra Verma for their assistance and construction of the new discriminant function diagrams. The authors also wish to thank Dr. Eyong John Takem for the field assistance.

## **References**

- [1] Dickinson, W.R., 1985 Interpreting provenance relations from detrital modes of sandstones. In: Zuffa, G.G. (ed) Provenance of Arenites. Dordrecht, Holland: Reidel, pp. 333–361. DOI: 10.1007/978-94-017-2809-6
- [2] Basu, A., Young, S.W., Suttner, L.J., James, W.C. and Mack, G.H., 1975. Re-evaluation of the use of undulatory extinction and polycrystallinity in detrital quartz for provenance interpretation: *J. sediment. Petrol.*, 45, 871-882. <https://doi.org/10.1306/212F6E6F-2B24-11D7-8648000102C1865D>
- [3] Bokanda, E.E., Ekomane, E., Kenfack, N.G.R., Njilah, K.I., Ashukem, N.E., Paul, T., Bisse S.B., Gabriel, N., Oroock, N.S., Belinga, B.C., 2019. Provenance, paleoclimate and diagenetic signatures of sandstones in the Mamfe Basin (West Africa). *Heliyon* 5 (2019) e01140. doi: 10.1016/j.heliyon.2019. e01140
- [4] Bhatia, M. R., 1983. Plate tectonics and geochemical composition of sandstone. *The Journal of Geology*,

91, 611-627.

- [5] Bhatia, M.R., Crook, K.A., 1986. Trace element characteristics of greywackes and tectonic setting discrimination of sedimentary basins. *Contributions to Mineralogy and Petrology*, 92, 181-193.
- [6] Weltje, G.J., 2012. Quantitative models of sediment generation and provenance: state of the art and future developments. *Sedimentary Geology* 280, 4–20.
- [7] Von Eynatten, H., Dunkl, I., 2012. Assessing the sediment factory: the role of single grain analysis. *Earth-Science Reviews* 115, 97–120.
- [8] Verma, S.P., Armstrong-Altrin, J.S., 2013. New multi-dimensional diagrams for tectonic discrimination of siliciclastic sediments and their application to Pre-Cambrian basins. *Chemical Geology*, 355, 117–180.
- [9] Verma, S.P., Armstrong-Altrin, J.S., 2016. Geochemical discrimination of siliciclastic sediments from active and passive margin settings. *Sedimentary Geology*, 332, 1-12.
- [10] Eyong, J.T., Wignall, P., Fantong, W.Y., Best, J., Hell, J.V., 2013. Paragenetic sequences of carbonate and sulphide minerals of the Mamfe Basin (Cameroon): Indicators of palaeo-fluids, palaeo-oxygen levels and diagenetic zones. *Journal of African Earth Sciences*, 86, 25–44.
- [11] Nguimbous-Kouoh, J.J., Takougam, E.M.T., Nouayou, R., Tabod, C.T., Manguelle-Dicoum, E., 2012. Structural Interpretation of the Mamfe Sedimentary Basin of Southwestern Cameroon along the Manyu River Using Audiomagnetotellurics. *Survey. Geophysics*, 7p
- [12] Bokanda, E.E., Ekomane, E., Eyong, J.T., Njilah, I.K., Ashukem, E.N., Bisong, R.N., Bisse, S.B., 2018a. Genesis of clastic dykes and soft sediment deformation Structures in the Mamfe Basin, South-West Region, Cameroon: Field Geology Approach. *Journal of Geological Research*. Volume 2018: 8
- [13] Bokanda, E.E., Ekomane, E., Fralick, P., Njilah, I.K., Bisse, S.B., Akono, D.F., Ekoa, B.A.Z., 2018b. Geochemical characteristics of shales in the Mamfe Basin, South West Cameroon: implication for depositional environments and oxidation conditions. *J. Afr. Earth Sci.* 149 (2019), 131e142.
- [14] Le Fur, 1965. Mission Socle-Cretacé, Rapport BRGM sur les indices de Pb/Zn du golfe de Mamfé
- [15] Abolo, M.G., 2008. Geology and petroleum potential of the Mamfe Basin, Cameroon, Central Africa, *Africa Geoscience Review. Special Publication*, 65–77.
- [16] Nguetchoua, G., Ekoa, B. A. Z., Eyong, T. J., Demanou, Z. D., Baba, D. H., Tchami, N. L. (2019). Geochemistry of cretaceous fine-grained siliciclastic rocks from Upper Mundeck and Logbadjeck Formations, Douala sub-basin, SW Cameroon: Implications for weathering intensity, provenance, paleoclimate, redox condition, and tectonic setting. *Journal of African Earth Sciences*. <https://doi.org/10.1016/j.jafrearsci.2019.02.021>

- [17] Ntokozo, M., Kuiwu, L., and Baojin, Z., 2013. Facies Analysis and depositional environments of the late Palaeozoic coal-bearing madzaringwe formation in the Tshipise-Pafuri Basin, South Africa. *Journal of geological research* Vol 2013, 11 p
- [18] Muhammad, M., Abdul Hadi, A.R., Chow, W.S., Zainey, K., 2018. Facies associations, depositional environments and stratigraphic framework of the Early Miocene-Pleistocene successions of the Mukah-Balingian Area, Sarawak, Malaysia, *Journal of Asian Earth Sciences* 152 23–38
- [19] Eyong, J.T., Nguetchoua, G., Bessong, M., Hell, J.V., Bokanda, E.E., Wignall, P., Best, J., 2018. Sedimentologic and palaeoenvironmental evolution of the Mamfe Cretaceous Basin (SW Cameroon): evidence from lithofacies analysis, tectonics and evaporate minerals suite. *Journal of African Earth Sciences*,149, 19–41.
- [20] Li, ZC., Li, W.H., Lai, S.C., Li, Y.X., Li, Y.H., Shang, T., 2015. The palaeosalinity analysis of Paleogene lutite in Weihe Basin. *Acta Sedimentol Sin.* 33(3):480–485 (in Chinese with English abstract)
- [21] Zhao, B.S., Jin, Z., Geng, Y., Wen, X., Yan, C., 2016b. Applying sedimentary geochemical proxies for paleoenvironment interpretation of organic-rich shale deposition in the Sichuan Basin, China. *Int J Coal Geol.* 163:52–71
- [22] Zhao, B.S., Li, R.X., Wang, X.Y., Wu, X.Y., Wang, N., Qin, X.I., Cheng, J.H., Li, J.J., 2016a. Sedimentary environment and preservation conditions of organic matter analysis of Shanxi Formation mud shale in Yanchang exploration area, Ordos Basin. *Geol. Sci. Technol. Inf.* 35(6):103–111 (in Chinese with English abstract)
- [23] Thomas, C.W., Aitchison, J., 2005. Compositional data analysis of geological variability and process: a case study. *Mathematical Geology* 37, 753–772.
- [24] Kröner, A. Stern, R.J., 2004. *Pan-African Orogeny*. Elsevier, Amsterdam, 1, 1-12.
- [25] Toteu, S.F., Penaye, J., Djomani, Y.P., 2004. Geodynamic evolution of the Pan-African belt in central Africa with special reference to Cameroon. *Canadian Journal of Earth science*, 41, 73-85.
- [26] Garver, J.I, Royce, P.R., Smick, T.A., 1996. Chromium and Nickel in Shale of the Taconic Foreland; a Case Study for the Provenance of Fine-Grained Sediments with an Ultramafic Source. *Journal of Sedimentary Research* 66:100–106. <https://doi.org/10.1306/D42682C5-2B26-11D7-8648000102C1865D>
- [27] Armstrong-Altrin, J.S., Lee, Y.I., Verma, S.P., Ramasamy, S., 2004. Geochemistry of sandstones from the upper Miocene Kudankulam Formation, southern India: Implications for provenance, weathering,

and tectonic setting: *Journal of Sedimentary Research*, 74(2), 285-297.

- [28] Cullers, R.L., 2002. Implications of elemental of elemental concentrations for provenance, redox conditions, and metamorphic studies of shales and limestone near Pueblo, CO, USA. *Chemical Geology*, 191, 305-327.
- [29] Delu, L., Rongxi, L., Zengwu, Z., Xiaoli, W., Futian, L., Bangsheng, Z., Jinghua, C., Baoping, W., 2017. Elemental characteristics and paleoenvironment reconstruction: a case
- [30] Xie, G., Shen, Y., Liu, S., Hao, W., 2018. Trace and rare earth element (REE) characteristics of mudstones from Eocene Pinghu Formation and Oligocene Huagang Formation in XihuSag, East China Sea Basin: Implications for provenance, depositional conditions and paleoclimate. *Marine and Petroleum Geology*. 1: 1-35.
- [31] Abigail, C.A., Balz, S.K., Malcolm, R.W., Ian, W., Isik K., 2010. Trace elements record depositional history of an Early Archean stromatolitic carbonate platform. *Chemical Geology*. 270, 148–163.